

# Boiling in micro-channels

G. HETSRONI\*

Department of Mechanical Engineering, Technion – Israel Institute of Technology, 32000, Haifa, Israel

**Abstract.** Boiling heat transfer in micro-channels is a subject of intense academic and practical interest. Though many heat transfer correlations have been proposed, most were empirically formulated from experimental data. However, hydrodynamic and thermal aspects of boiling in micro-channels are not well understood. Moreover, there are only a few theoretical models that link the heat transfer mechanism with flow regimes in micro-channels. Also, there are discrepancies between different sets of published results, and heat transfer coefficients have either well exceeded, or fallen far below, those predicted for conventional channels. Here we consider these problems with regard to micro-channels with hydraulic diameters ranging roughly from 5  $\mu\text{m}$  to 500  $\mu\text{m}$ , to gain a better understanding of the distinct properties of the measurement techniques and uncertainties, the conditions under which the experimental results should be compared to analytical or numerical predictions, boiling phenomenon, as well as different types of micro-channel heat sinks. Two-phase flow maps and heat transfer prediction methods for vaporization in macro-channels are not applicable in micro-channels, because surface tension dominates the phenomena, rather than gravity forces. The models of convection boiling should correlate the frequencies, sizes and velocities of the bubbles and the coalescence processes, which control the flow pattern transitions, together with the heat flux and the mass flux. Therefore, the vapour bubble size distribution must be taken into account. The flow pattern in parallel micro-channels is quite different from that in a single micro-channel. At same values of heat and mass flux, different, time dependent, flow regimes occur in a given micro-channel. At low vapour quality, heat flux causes a sudden release of energy into the vapour bubble, which grows rapidly and occupies the entire channel cross section. The rapid bubble growth pushes the liquid-vapour interface on both caps of the vapour bubble, at the upstream and the downstream ends, and leads to a reverse flow. We term this phenomenon as explosive boiling. One of the limiting operating conditions with flow boiling is the critical heat flux (CHF). The CHF phenomenon is different from that observed in conventional size channels.

**Key words:** micro-channel, boiling, pressure drop, heat transfer, fluctuation.

## 1. Introduction

To achieve higher heat dissipation rates for micro-electronic and optical technologies, the fundamentals of two-phase heat transfer in micro-channels are being studied ever more extensively. Micro-channel heat sinks are devices that provide liquid or two-phase flow through parallel channels of diameter less than, say, 1 mm. These systems are ideally suited for devices where high heat flux is dissipated from small surface area of high performance supercomputers, optical devices, electric vehicles and advanced military avionics. The hydraulic diameter of micro-channels,  $d_h$ , is in the range 10–500  $\mu\text{m}$ , the length,  $L$ , is in the range 10–15 mm.

Qu and Mudawar [1] presented and discussed experimental results, which provide physical insight into the unique nature of saturated flow boiling heat transfer in a water-cooled micro-channel heat sink. Contrary to macro-channel the heat transfer coefficient was shown to decrease with increasing thermodynamic equilibrium quality. This unique trend was attributed to appreciable droplet entrainment and onset of annular flow regime. Such a trend was also reported by Hetsroni et al. [2]. On the other hand, Bertsch et al. [3] found that heat transfer coefficient first rises steeply as vapour quality increases from a subcooled value, and again drops sharply with further increases in vapour quality. Agostini et al. [4] presented experimental results on flow boiling of refrigerants R236fa and R245fa in silicon heat sinks. Three significant

heat transfer trends were identified: the heat transfer coefficient was independent of the heat flux, increased or decreased with heat flux.

An annular flow model was developed by Qu and Mudawar [5] to predict the saturated flow boiling heat transfer coefficient. Laminar liquid and vapor flow, smooth interface, and strong droplet entrainment and deposition effects were incorporated into the model.

Kandlikar and Balasubramanian [6] presented the flow boiling correlations to transition, laminar and deep laminar flows in micro-channels. The flow boiling correlations for large diameter tubes were modified for flow boiling in micro-channels. It was concluded that boiling was more nucleate dominant for low Reynolds numbers ( $Re < 100$ ) in micro-channels. Thome et al. [7] proposed a new heat transfer model for evaporation in the elongated-bubble regime in micro-channels. The model describes the transient variation in local heat transfer coefficient during the sequential and cyclic passage of a liquid slug, an evaporating elongated bubble and a vapour slug. The time averaged local heat transfer coefficient calculated using this model was compared by Dupont et al. [8] to 1591 experimental data which cover tube diameters from 0.77 to 3.1 mm. The data were obtained for the following seven fluids: R-11, R-12, R-113, R-123, R-134a, R-141b, and  $\text{CO}_2$ . The new model predicts 67% of the database to within  $\pm 30\%$ .

\*e-mail: hetsroni@technix.technion.ac.il

Zhang et al. [9] proposed a correlation for flow boiling heat transfer in mini-channels. However, the realistic prediction of flow boiling heat transfer coefficients is possible only for a set of experimental data selected by the authors of these models. For example, the mean relative error of prediction of recent experimental data presented by Agostini et al. [4] by different investigations is: Thome et al. [7] +4%, Kandlikar and Balasubramanian [6] –23%, Lee and Mudawar [10] –609%, Zhang et al. [9] +35%.

An important aspect of flow boiling in micro-channels is the pressure fluctuations, because these fluctuations can lead to instabilities in flow. Pressure fluctuations and corresponding temperature oscillations are associated with boiling in micro-channels to a greater extent than in conventional channels. This is because the flow velocities are very low, and bubble formation can cause a significant disruption of low-quality flow. The periodic wetting and rewetting phenomena were observed by Hetsroni et al. [2, 11–13], Zhang et al. [14], Steinke and Kandlikar [15]. The explosive vaporization and significant pressure drop fluctuations were observed by Hetsroni et al. [2, 12]. Flow pattern, observed in these studies and reported also by Kandlikar [16], revealed a flow reversal in some channels with expanding bubbles pushing the liquid–vapor interface in both upstream and downstream directions. Lee et al. [17, 18] studied experimentally bubble dynamics in a single trapezoid micro-channel and in two parallel micro-channels with a hydraulic diameter of 41.3  $\mu\text{m}$ . Bubble nucleation and growth in parallel micro-channels were observed for some cases with the wall temperature lower than the saturation temperature corresponding to the system pressure. It was reported by Bergles and Kandlikar [19] that CHF in micro-channels under conditions of low mass flux and low quality may be a result of instabilities rather than conventional dryout mechanism.

The main purpose of the present study is to highlight the dynamics of vapour bubble, and heat transfer coefficient under condition boiling regime in micro-channels.

## 2. Dynamics of vapor bubble

The bubble dynamics in a confined space, in particular in micro-channels, is quite different from that in unconfined still fluid. In micro-channels the bubble evolution depends on a number of different factors such as existence of solid walls restricting bubble expansion in the transversal direction, a large gradient of the velocity and temperature field, etc. Some of these problems were discussed by Kandlikar [16], and Dhir [20]. A detailed experimental study of bubble dynamics in a single and two parallel micro-channels was performed by Lee et al. [21] and Li et al. [22].

**2.1. Dimensional analysis.** Yarin et al. [23] presented the functional equation for the rate of bubble growth as follows

$$\frac{dr}{dt} = f(q, h_{LG}, \rho_L, \rho_G, \mu_L, k_L, c_{pL}, d_0, d_*, \sigma, \Delta T_S, g, t, U), \quad (1)$$

where  $dr/dt$  is the rate of bubble growth,  $t$  is the time.

Among the dimensional variables of the problem, five parameters which have independent dimensions may be chosen, and then Eq. (1) may be written in dimensionless form. Choosing parameters  $\rho_L$ ,  $c_{pL}$ ,  $U$ ,  $\Delta T_S$ ,  $d_*$  and taking into account the  $\pi$ -theorem, Eq. (1) can be represented as:

$$\Pi = \phi(\Pi_1, \Pi_2, \dots, \Pi_9), \quad (2)$$

where

$$\Pi = \frac{\dot{r}}{U}, \quad \Pi_1 = \frac{q}{\rho_L U c_{pL} \Delta T_S},$$

$$\Pi_2 = \frac{h_{LG}}{c_{pL} \Delta T_S}, \quad \Pi_3 = \frac{\rho_G}{\rho_L},$$

$$\Pi_4 = \frac{\mu_L}{\rho U d_*}, \quad \Pi_5 = \frac{k_L}{\rho_L c_{pL} U d_*},$$

$$\Pi_6 = \frac{d_0}{d_*}, \quad \Pi_7 = \frac{\sigma}{\rho U^2 d_*},$$

$$\Pi_8 = \frac{g d_*}{U^2}, \quad \Pi_9 = \frac{\tau U}{d_*},$$

$$\dot{r} = \frac{dr}{dt}.$$

Analysis of experimental data presented by Lee et al. [21] revealed that the parameters  $\Pi_3 - \Pi_9$  did not change significantly, and the parameter  $\Pi_2$  depends mainly on the wall access temperature,  $\Delta T_S = T_W - T_S$ . We assumed that  $\Pi_2 \approx \text{const}$ . Thus, one can consider  $\Pi_1$  as the dimensionless parameter that determines the rate of bubble growth in the linear regime:

$$\frac{dr}{dt} = \phi(\Pi_1). \quad (3)$$

**2.2. Experimental data. Single micro-channel.** Data by Lee et al. [21] and Li et al. [22] contain the results related to bubble dynamics in a single micro-channel.

In the range of  $\Pi_1 = 0.00791 - 0.0260$  linear behaviour of the bubble radius was observed, when  $\Pi_1 > 0.0260$  exponential bubble growth took place (Fig. 1).

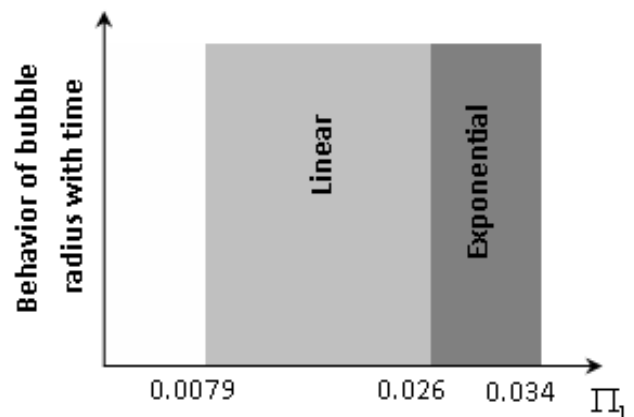


Fig. 1. Behaviour of bubble change of radius vs. time. The values of  $\Pi_1$  were calculated from experimental data

**2.3. Parallel micro-channels.** The bubble dynamics under conditions corresponding to flow in two parallel trapezoidal micro-channels with hydraulic diameter  $47.7 \mu\text{m}$  was studied by Li et al. [22]. The bubbles in two parallel micro-channels generally grow in a similar way to that in a single micro-channel. The authors also reported the presence of two-phase flow instability.

Hetsroni et al. [11] studied bubble growth in 26 parallel horizontal triangular micro-channels of  $d_h = 103 \mu\text{m}$  and length of 10 mm. Temporal variation of bubble size is shown in Fig. 2. Figures 2a, b show the variation of bubble size in the streamwise direction  $L_p$ , and in the spanwise direction  $L_n$ , respectively.

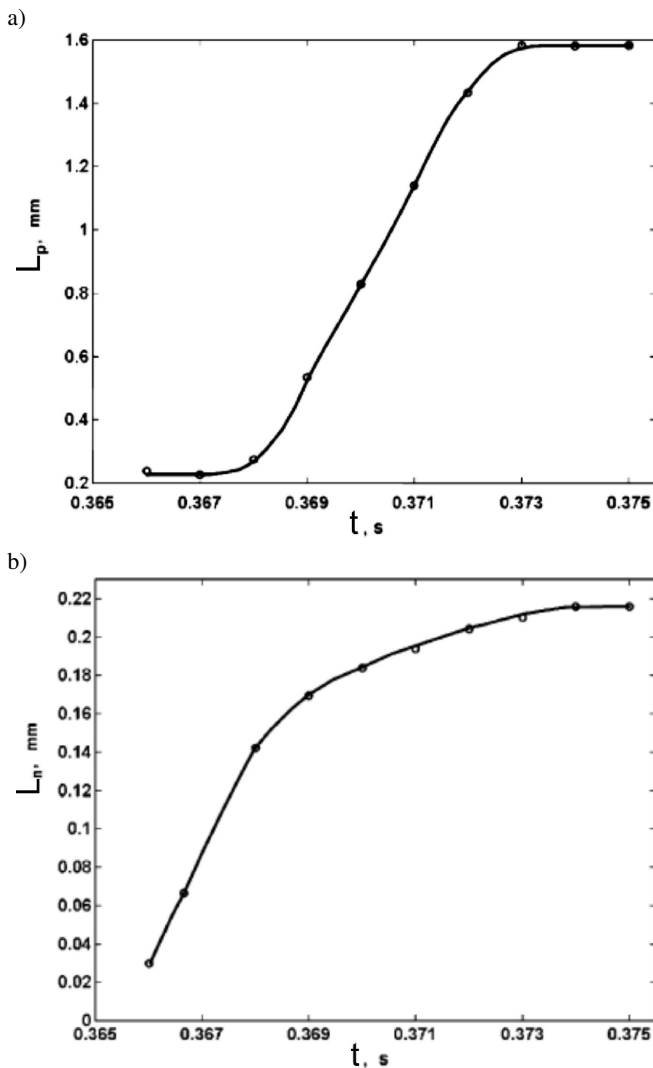


Fig. 2. Temporal variation of vapour bubble size: a) streamwise direction,  $L_p$  b) spanwise direction,  $L_n$ .  $U_{LS} = 0.046 \text{ m/s}$ ,  $q = 8 \times 10^4 \text{ w/m}^2$

The observed ratio  $f = L_p/L_n$ , is quite different from that reported for subcooled flow boiling of water in tubes of 17–22 mm inner diameter. Prodanovic et al. [24] reported that this ratio was typically around 0.8 for experiments at 1.05–3 bar.

**2.4. Bubble velocity.** Figure 3 shows the velocity of the displacement of the bubble tail in the streamwise direction  $U_b$  (m/s) versus the bubble lifetime  $t$ , at fixed conditions as described above, i.e.,  $q = 8 \times 10^4 \text{ W/m}^2$ ,  $U_{LS} = 0.046 \text{ m/s}$ . One may conclude that the velocity of bubble displacement varies, depending on the range of lifetime. In region A of the boiling process, during the period of about 0.005 s from the appearance of the first bubble, ONB, the bubble velocity is equal to the superficial liquid velocity. It should be noted that the term ONB, known as the onset of nucleate boiling, was borrowed from the terminology of subcooled flow boiling in larger tubes. Region B is characterized by a sharp increase in the bubble velocity, namely the bubble is accelerated in the streamwise flow direction. Figure 3 shows that in this region the bubble velocity increases about threefold, during a time interval of about 0.003 s. After the time when  $U_b$  reaches maximum value it remains constant, as shown in Fig. 3, region C.

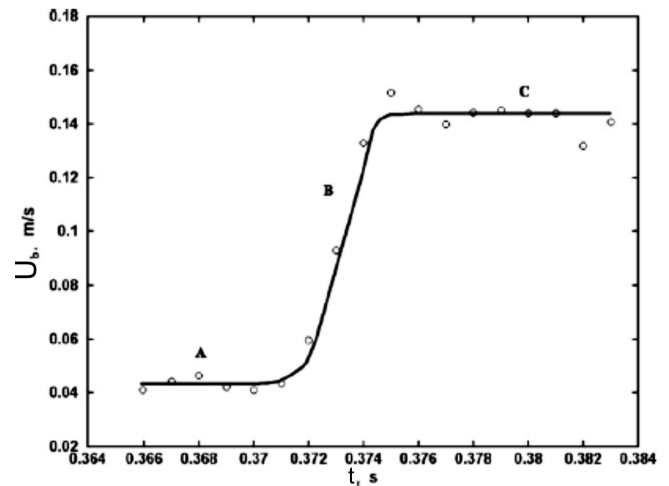


Fig. 3. The velocity of bubble displacement.  $U_{LS} = 0.046 \text{ m/s}$ ,  $q = 80 \text{ kW/m}^2$

Such a behaviour agrees with results reported by Agostini et al. [25]. The collision of elongated bubble has been studied by Revellin et al. [26] along adiabatic glass micro-channels of 509 and 709  $\mu\text{m}$  internal diameters for refrigerant R-134 a. A model for the collision of elongated bubbles in micro-channels was proposed to predict the bubble length distribution at the exit of the micro-evaporator.

In micro-channels, bubbles cause a significant volume change (relative to the channel size). As a result, pressure fluctuations were observed. The temporal behaviour of the pressure drop is shown in Fig. 4.

The pressure spike introduces a disruption in the flow. Depending on the local conditions, the excess pressure inside the bubble may overcome the inertia of the incoming liquid and the pressure in the inlet manifold, and cause a reverse flow of varying intensity, depending on the local conditions. There are two ways to reduce the flow instabilities: reduce the local liquid superheat at the ONB and introduce a pressure drop element at the entrance of each channel, Kandlikar [27]. Kakac and Bon [28] reported that density-wave oscillations

were observed also in conventional size channels. Introduction of additional pressure drop at the inlet (small diameter orifices were employed for this purpose) stabilized the system.

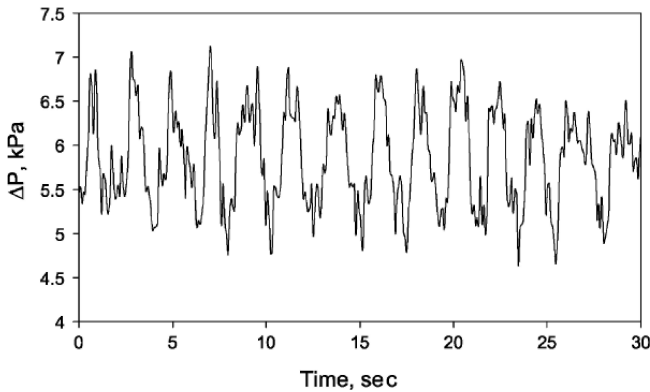


Fig. 4. Pressure drop fluctuations.  $U_{LS} = 0.14$  m/s,  $q = 220$  kW/m<sup>2</sup>

Simultaneous visualizations and measurements were done by Wang et al. [29] to investigate effects of inlet/outlet configurations on flow boiling instabilities in parallel micro-channels having a length of 30 mm and a hydraulic diameter of 186  $\mu$ m. It was found that nearly steady flow boiling existed in the parallel micro-channels through an inlet restriction.

### 3. Heat transfer

The heat transfer coefficient of boiling flow through a horizontal rectangular channel with low aspect ratio (0.02–0.1) was studied by Lee and Lee [30]. The detail experimental study of flow boiling heat transfer in two-phase heat sinks was performed by Qu and Mudawar [5]. It was shown that the saturated flow boiling heat transfer coefficient in a micro-channel heat sink is a strong function of mass velocity and depends only weakly on the heat flux. This result, as well as the results by Lee and Lee [30], indicates that the dominant mechanism for water micro-channel heat sinks is forced convective boiling but not nucleate boiling.

Heat transfer characteristics for saturated boiling were considered by Yen et al. [31]. From this study of convective boiling of HCFC123 and FC72 in micro-tubes with inner diameter 190, 300 and 510  $\mu$ m one can see that in the saturated boiling regime, the heat transfer coefficient monotonically decreased with increasing vapour quality, but is independent of mass flux.

The convective and nucleate boiling heat transfer coefficient was the subject of experiments by Grohmann [32]. The measurements were performed in micro-tubes of 250 and 500  $\mu$ m in diameter. Nucleate boiling metastable flow regimes were observed. Heat transfer characteristics at the nucleate and convective boiling in micro-channels with different cross-sections were studied by Yen et al. [33].

Several popular macro-channel correlations, and recently recommended small-channel correlations, were examined by Lee and Mudawar [34]. Predictions were adjusted for the three-sided wall heating and rectangular geometry.

Experiments by Lee and Mudawar [34] reveal the range of parameters at which heat transfer is controlled by nucleate boiling or annular film evaporation. The first of these processes occurs only at low qualities ( $x < 0.05$ ) corresponding to very low heat fluxes; the second one at moderate ( $0.05 < x < 0.55$ ) or high ( $x > 0.55$ ) qualities that correspond to higher heat fluxes. New correlations were suggested by Lee and Mudawar [34]. They are based on the Martinelli parameter  $X$  and account for micro-channel effects not represented in the prior correlations.

The work by Steinke and Kandlikar [15] focused on obtaining heat transfer data during flow boiling in micro-channels. An experimental investigation was performed for flow boiling using water in six parallel, horizontal micro-channels with a hydraulic diameter of 207  $\mu$ m. The ranges of parameters are: mass flux from 157 to 1782 kg/m<sup>2</sup>s, heat flux from 5 to 930 kW/m<sup>2</sup>, inlet temperature of 22°C, quality from sub-cooled to 1.0, and atmospheric pressure at the exit.

$$h_{tp} = 0.6683Co^{-0.2}(1-x)^{0.8}f_2h_L + 1058Bo^{0.7}(1-x)^{0.8}F \cdot h_L, \quad (4)$$

$$Co = \left(\frac{\rho_G}{\rho_L}\right)^{0.5} \left(\frac{1-x}{x}\right)^{0.8}, \quad (5)$$

$$Bo = \frac{q}{Gh_{LG}}, \quad (6)$$

where  $Co$  is the convection number given in Eq. (5),  $Bo$  is the boiling number given in Eq. (6),  $f_2$  is the multiplier,  $h_L$  is the heat transfer coefficient with all liquid flow, and  $x$  is the quality. The  $F$  number for water is 1.0 and the  $f_2$  is multiplier is 1.0 for micro-channel flow.

The empirical correlation obtained by Steinke and Kandlikar [15] predicts a heat transfer coefficient about twice higher than that measured by Qu and Mudawar [5] during flow boiling of water ( $x < 0.15$ ) and during flow boiling of R-134a ( $x = 0.4$ –0.8). This correlation also overpredicts the experimental data obtained by Yen et al. [31] during convective boiling of HCFC123 and FC72 in  $d = 190$   $\mu$ m tubes in the range of  $x = 0.4$ –0.9.

**3.1. Critical heat flux of flow boiling.** Zhang et al. [35] proposed a correlation for CHF under condition of saturated boiling:

$$Bo = 0.0352 \left[ We + 0.0119 \left(\frac{L}{d_h}\right)^{2.31} \left(\frac{\rho_G}{\rho_L}\right)^{0.361} \right]^{-0.295} \times \left[ \left(\frac{L}{d_h}\right)^{-0.311} \left(2.05 \left(\frac{\rho_L}{\rho_L}\right)^{0.170} - x_{in}\right) \right], \quad (7)$$

where  $Bo = q_{crit}/(h_{LG}G)$  is the boiling number,  $We = (G^2d_h)/(\sigma\rho_L)$  is the Weber number,  $q_{crit}$  is the critical heat flux,  $h_{LG}$  is the latent heat of vaporization,  $G$  is the mass flux,  $x_{in}$  is the thermodynamic equilibrium quality at the inlet,  $\rho_G$  and  $\rho_L$  are the densities of saturated vapor and liquid, respec-

tively,  $d_h$  is the hydraulic diameter,  $L$  is the heated length, and  $\sigma$  is the surface tension.

Hall and Mudawar [36] provided a comprehensive review of the current state of knowledge of subcooled CHF for water flow boiling in channels, and proposed a statistical correlation with five parameters based on almost all available subcooled CHF databases in the literature:

$$Bo = \frac{C_1 We^{C_2} (\rho_L / \rho_G)^{C_3} [1 - C_4 (\rho_L / \rho_G)^{C_5} x_{in}]}{1 + 4C_1 C_4 We^{C_2} (\rho_L / \rho_G)^{C_3 + C_5} (L / d_h)} \quad (8)$$

where the Weber number  $We = G^2 d_h / (\rho_L \sigma)$ ,  $C_1 = 0.0722$ ,  $C_2 = 0.312$ ,  $C_3 = 0.644$ ,  $C_4 = 0.900$ , and  $C_5 = 0.724$ . The correlation was developed using a total of 4860 data points and predicted CHF with a rms error of 14.3% in the following parametric ranges:  $0.1 < P_0 < 20$  MPa,  $0.25 < d_h < 15.0$  mm,  $2 < L/d_h < 200$ ,  $300 < G < 30000$  kg/m<sup>2</sup> s,  $2.00 < x_{in} < 0.00$ , and  $1.00 < x_{out} < 1.00$ .

A theoretical model for the prediction of the critical heat flux of refrigerants flowing in heated, round micro-channels has been developed by Revellin and Thome [26]. The model is based on the two-phase conservation equations and includes the effect of the height of the interfacial waves of the annular film. Validation has been performed by comparing the model with experimental results presented by Wojtan et al. [37], Qu and Mudawar [38], Bowers and Mudawar [39], Lazareck and Black [40]. More than 96% of the data for water and R-113, R-134a, R245fa were predicted within  $\pm 20\%$ .

**3.2. Explosive boiling of water in parallel micro-channels.** The thermo-hydrodynamic processes of boiling in a micro-channel heat sink were subject to a number of experimental investigations performed during the last decade. Periodic wetting and rewetting phenomena were observed by Hetsroni et al. [11, 12], Zhang et al. [14], Steinke and Kandlikar [15], and Kandlikar and Balasubramanian [6].

**3.3. Quasi-periodic boiling in a certain single micro-channel of a heat sink.** The main parameters that affect the explosive boiling oscillations (EBO) in an individual channel of a heat sink such as hydraulic diameter, mass flux, and heat flux were studied by Hetsroni et al. [11–13].

**3.4. Period between successive events.** Figure 5 shows the dependence of the dimensionless period of phase transformations (i.e., the time between bubble venting),  $t^*$ , on boiling number  $Bo$  ( $t^* = t/Ud_h$ ,  $Bo = q/Gh_{LG}$ , where  $t$  is the period between successive events,  $U$  is the mean velocity of single-phase flow in the micro-channel,  $d_h$  is the hydraulic diameter of the channel,  $q$  is heat flux,  $m$  is mass flux,  $h_{LG}$  is the latent heat of vaporization). The dependence of  $t^*$  on  $Bo$  can be approximated, with a standard deviation of 16%, by

$$t^* = 0.000030 Bo^2 \quad (9)$$

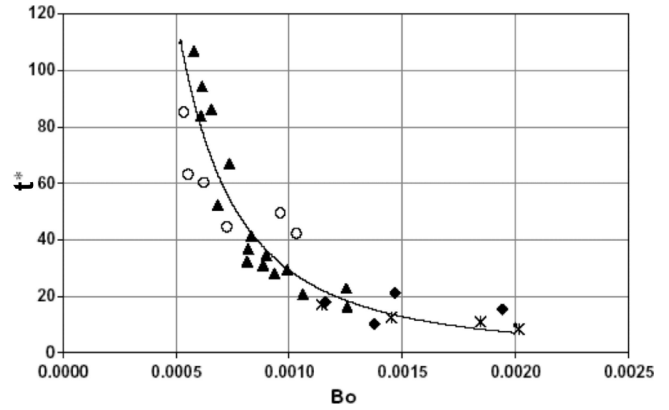


Fig. 5. The dependence of the dimensionless time interval between cycles on the boiling number: circles (o) represent  $d_h = 100 \mu\text{m}$ , water, triangles (▲) represent  $d_h = 130 \mu\text{m}$ , water, diamonds (◆) represent  $d_h = 220 \mu\text{m}$ , water, star (\*) represents  $d_h = 220 \mu\text{m}$ , ethanol

**3.5. The initial thickness of the liquid film.** The term initial liquid film thickness is defined as the average thickness of fluid, evenly distributed during the period  $t$ , over the surface of the circular micro-channel, after venting of the elongated bubble.

The average liquid thickness  $\delta$ , can be calculated as:

$$\delta = qt / \rho_L h_{LG}. \quad (10)$$

Figure 6 shows the dependence of the dimensionless initial liquid thickness of water and ethanol  $\delta^*$ , on the boiling number  $Bo$ , where  $\delta^* = \delta U / \nu$ ,  $U$  is the mean velocity of single-phase flow in the micro-channel, and  $\nu$  is the kinematic viscosity of the liquid at saturation temperature. The dependence of  $\delta^*$  on  $Bo$  can be approximated, with a standard deviation of 18%, by:

$$\delta^* = 0.00015 Bo^{-1.3}. \quad (11)$$

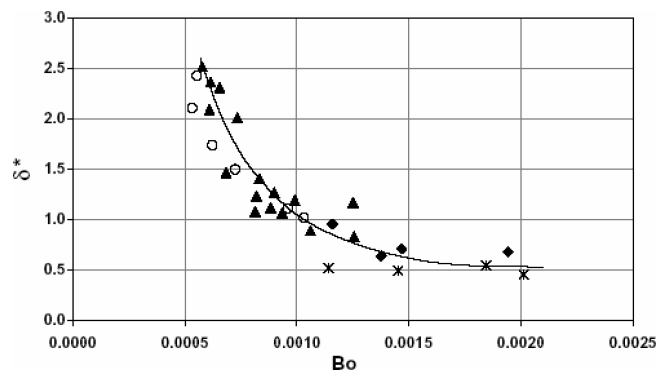


Fig. 6. Dependence of the dimensionless initial film thickness on the boiling number: circles (o) represent  $d_h = 100 \mu\text{m}$ , water, triangles (▲) represent  $d_h = 130 \mu\text{m}$ , water, diamonds (◆) represent  $d_h = 220 \mu\text{m}$ , water, star (\*) represents  $d_h = 220 \mu\text{m}$ , ethanol

The initial thickness of the liquid film is a key parameter of the explosive boiling. The term initial liquid film thickness is defined as the average thickness of fluid, evenly distributed during period  $t$ , over the surface of the circular micro-channel,

after venting of the elongated bubble. This surface is located downstream of the ONB and may be characterized by the heated length and hydraulic diameter. This point may be discussed in some detail with regard to the beginning of the critical heat flux (CHF) regime. The variation of the initial thickness of the film of water versus the heat flux is depicted in Fig. 7. For explosive boiling the film thickness decreases with increasing heat flux from 125 to 270 kW/m<sup>2</sup> from about 8 to 3 μm. This range of values is on the same order of magnitude as those given by Moriyama and Inoue [41] and by Thome et al. [7] for R-113 in small spaces (100–400 μm). Decreasing liquid film thickness with increasing heat flux is a distinct feature of dryout during explosive boiling. Under the conditions at which the instantaneous temperature of the heater surface exceeds 125°C, the value of  $\delta$  was in the range of 3–0.6 μm. This value may be considered as minimum initial film thickness. If the liquid film reached the minimum initial film thickness  $\delta_{\min}$ , CHF regime occurred. According to Thome et al. [7]  $\delta_{\min}$  is assumed to be on the same order of magnitude as the surface roughness. The values of the minimum initial film thickness calculated by Thome et al. [7] for R-113 at saturation temperature 47.2°C was in the range of 1.5–3.5 μm.

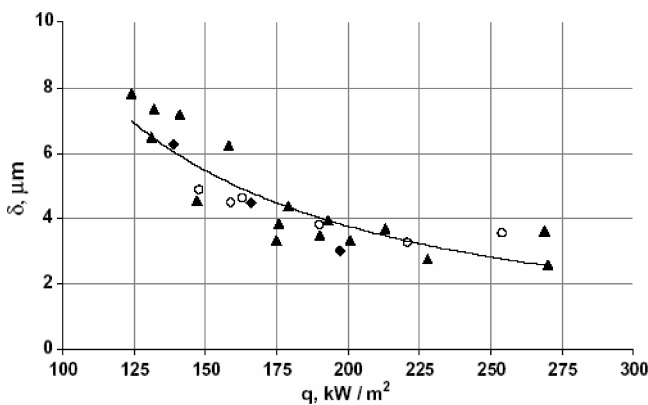


Fig. 7. The variation of the initial film thickness for water versus heat flux: circles (○) represent  $d_h = 100 \mu\text{m}$ , water, triangles (▲) represent  $d_h = 130 \mu\text{m}$ , water, diamonds (◆) represent  $d_h = 220 \mu\text{m}$ , water

**3.6. System that contains a number of parallel micro-channels.** Hetsroni et al. [11–13] also studied the effect of EBO in individual channels on the average characteristics of the whole heat sink: total pressure drop and temperature fluctuations on the heater, and the heat transfer coefficient. The high-frequency oscillations in individual micro-channels are superimposed and lead to total low-frequency pressure drop and temperature oscillations of the system.

**Fluctuation of pressure drop, fluid and heated wall temperatures.** The experimental investigations of boiling instability in parallel micro-channels were carried out by simultaneous measurements of temporal variations of pressure drop, fluid and heater temperatures. The channel-to-channel interactions may affect pressure drop between the inlet and the outlet manifold as well as associated temperature of the fluid in the outlet manifold and heater temperature. Figure 8

illustrates this phenomenon for pressure drop in the heat sink that contains 13 micro-channels of  $d_h = 220 \mu\text{m}$  at mass flux  $G = 93.3 \text{ kg/m}^2\text{s}$  and heat flux  $q = 200 \text{ kW/m}^2$ . The temporal behaviour of the pressure drop in the whole boiling system is shown in Fig. 8a. The considerable oscillations were caused by the flow pattern alternation, that is, by the liquid/two-phase alternating flow in the micro-channels. The pressure drop FFT is presented in Fig. 8b. Under condition of the given experiment, the period of pressure drop fluctuation is about  $t = 0.36 \text{ s}$ .

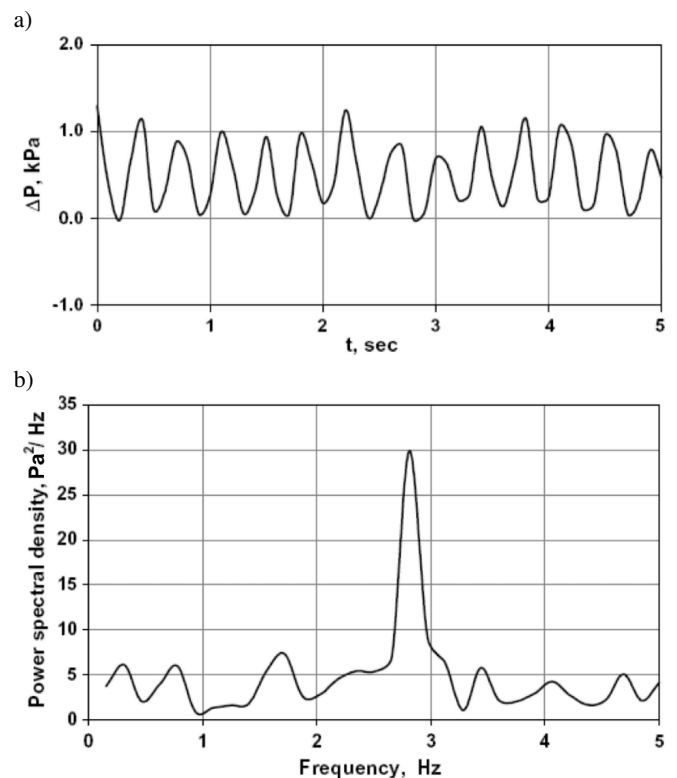


Fig. 8. Time variation of pressure drop at  $q = 200 \text{ kW/m}^2$ : a) pressure drop fluctuations, b) pressure drop amplitude spectrum

The pressure drop fluctuation provides an insight into the temperature behaviour of the fluid in the outlet manifold. The pressure drop fluctuation frequency represents the oscillations in the system. Figure 9a, b shows the time variation and FFT of the fluctuation component of the fluid temperature. In Fig. 9a one can observe that the average fluid temperature at the outlet manifold is less than the saturation temperature. This results in the fact that only single liquid comes to the outlet manifold through some of the parallel micro-channels.

The time variation of the mean and maximum heater temperature is presented in Fig. 10. The mean heater temperature (i.e., the average temperature of the whole heater) changed in the range of  $\Delta T_{av} = 10 \text{ K}$ . The maximum heater temperature changed in the range of  $\Delta T_{\max} = 6 \text{ K}$ . Comparison between Figs. 8 and 9, shows that the time period (frequency) is the same for the pressure drop and the fluid temperature at the outlet manifold, and the mean and maximum heater temperature fluctuations. It also allows one to conclude that these

fluctuations are in phase. When the heat flux is increased, at constant value of mass flux, the oscillation amplitudes of the pressure drop, the fluid and the heater temperatures also increase.

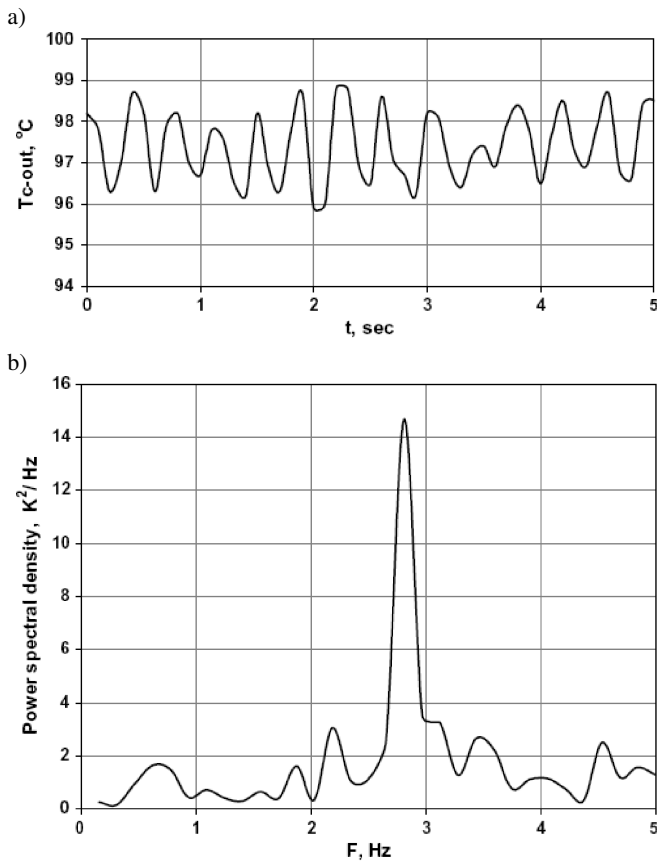


Fig. 9. The Time variation of the fluid temperature at the outlet manifold  $q = 200 \text{ kW/m}^2$ : a) temperature fluctuations, b) temperature amplitude spectrum 0.1

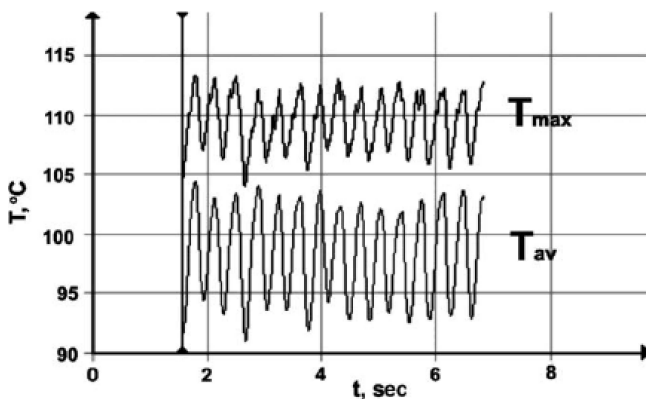


Fig. 10. Time variation of average and maximum heater temperature at  $q = 200 \text{ kW/m}^2$

**3.7. Average heat transfer coefficient.** In the range of quality  $x = 0.01\text{--}0.08$  it was observed that at the same boiling number and inlet temperature, an increase in diameter shifts the ONB further from the inlet. The region of the local dry-out decreases and the average heated surface temperature de-

creases as well. Under this condition the heat transfer coefficient increases with increased hydraulic diameter. In order to take into account the effect of surface tension and micro-channel hydraulic diameter, we have applied the Eotvos number  $Eo = g(\rho_L \rho_G) d_h^2 / \sigma$ . Figure 11 shows the dependence of the  $Nu/Eo$  on the boiling number  $Bo$ , where  $Nu = h d_h / k_L$  is the Nusselt number,  $h$  is the heat transfer coefficient, and  $k_L$  is the thermal conductivity of fluid. All fluid properties are taken at the saturation temperature. This dependence can be approximated, with a standard deviation of 18%, by the relation:

$$Nu/Eo = 0.030 Bo^{1.5}. \quad (12)$$

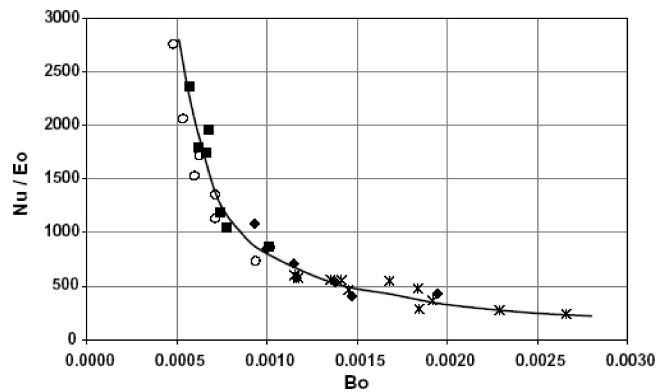


Fig. 11. The dependence of  $Nu/Eo$  on the  $Bo$ : circles (o) represent  $d_h = 100 \mu\text{m}$ , water, triangles (▲) represent  $d_h = 130 \mu\text{m}$ , water, diamonds (◆) represent  $d_h = 220 \mu\text{m}$ , water, star (\*) represents  $d_h = 220 \mu\text{m}$ , ethanol

## 4. Conclusions

**4.1. Bubble dynamics in a confined space.** Dimensional analysis shows that the variation of the bubble radius with time depends on the parameter  $\Pi = q / (\rho_L U c_{pL} \Delta T_S)$ . In the range of  $\Pi = 0.0079\text{--}0.026$ , linear behaviour was observed, and when  $\Pi > 0.026$  exponential bubble growth took place.

**Heat transfer in two-phase flow boiling.** The extent to which an incoming liquid will be vaporized is a design variable that depends on the intended application. In micro-scale refrigeration systems, the change in vapour quality may be substantial, on the order of 0.8 for example. In electronics cooling applications, the equilibrium vapour quality may remain at 0, or be very small; in those designs, the aim is to capture the high-heat transfer coefficients of subcooled flow boiling, without the added complexities of net vapour generation (e.g., the need to incorporate a condenser). The distinction between low and high-quality outflow affects heat transfer coefficients. Experiments by Lee and Mudawar [34] revealed the range of parameters at which heat transfer was controlled by nucleate boiling or annular film evaporation. The first of these processes occurred only at low qualities ( $x < 0.05$ ), the second one at moderate ( $0.05 < x < 0.55$ ) or high ( $x > 0.55$ ) qualities. New correlations were suggested by Lee and Mudawar [34]. They are based on the Martinelli parameter and may be used for two-phase flow boiling of water and refrigerant R-134a.

**4.2. Critical Heat Flux.** Several thousand CHF points have been reported in the boiling literature of the past 50 years. Most of these data were obtained with stable flow in single conventional size circular tubes and conventional size channels. The tubes were usually of uniform wall thickness, and direct electrical heating was utilized to simulate the constant heat flux. The correlation suggested by Zhang et al. [35], (Eq. (7)) gives the best agreement with experimental data on saturated CHF in channels of 0.33–6.22 mm. There is a significant difference between experimental results of CHF obtained in a single micro-channel of  $d_h = 0.5$  mm and in the block that contained twenty-one  $0.215 \times 0.21$  mm channels.

The study of CHF in micro-channels has not received much attention in the literature. Single-tube CHF data are not available for micro-channels with hydraulic diameters less than 0.3 mm. Under conditions of explosive boiling, Hetsroni et al. [13] suggested that the initial thickness of the liquid film may be considered as a key parameter that affects CHF in the system containing a number of parallel micro-channels of  $d_h = 0.1$ –0.22 mm. New experiments should be performed to validate the dimensionless groups suggested for the evaporating interface near the heated wall and CHF for single micro-channels, as well as for blocks that contain parallel micro-channels.

**4.3. Flow instability.** The channel-to-channel interactions may affect pressure drop between the inlet and the outlet manifolds, as well as associated temperature of the fluid in the outlet manifold and the temperature of the heater. The frequency and the phase are the same for all these fluctuations. They increase at a constant value of mass flux with increasing heat flux. The large heated wall temperature fluctuations are associated with CHF. As the heat flux approached CHF, the parallel-channel instability, which was moderate over a wide range of heat fluxes, became quite intense and must be associated with maximum temperature fluctuation of the heated surface.

## REFERENCES

- [1] I. W. Qu and I. Mudawar, "Measurement and prediction of pressure drop in two-phase micro-channel heat sinks", *Int. J. Heat Mass Transfer* 46, 2737–2753 (2003).
- [2] G. Hetsroni, A. Mosyak, Z. Segal, and G. Ziskind, "A uniform temperature heat sink for cooling of electronic devices", *Int. J. Heat Mass Transfer* 45, 3275–3286 (2002).
- [3] S.S. Bertsch, E.A. Groll, and S.V. Garimella, "Refrigerant flow boiling heat transfer in parallel micro-channels as a function of local vapor quality", *Int. J. Heat Mass Transfer* 51, 4775–4787 (2008).
- [4] B. Agostini, R. Revellin, and J. Thome, "Elongated bubbles in micro-channels. Part I: Experimental study and modeling of elongated bubble velocity", *Int. J. Multiphase Flow* 34, 590–601 (2008).
- [5] W. Qu and I. Mudawar, "Flow boiling heat transfer in two-phase micro-channel heat sink. I: Experimental investigation and assessment of correlation methods", *Int. J. Heat Mass Transfer* 46, 2755–2771 (2003).
- [6] S.G. Kandlikar and P. Balasubramanian, "An extension of the flow boiling correlation to transition, laminar and deep laminar flows in mini-channels and micro-channels", *Heat Transfer Eng.* 25, 86–93 (2004).
- [7] J.R. Thome, V. Dupont, and A.M. Jacobi, "Heat transfer model for evaporation in micro-channels. Part I: Comparison with database", *Int. J. Heat Mass Transfer* 47, 3375–3385 (2004).
- [8] V. Dupont, J.R., Thome, and A.M., Jacobi, "Heat transfer model for evaporation in micro-channels. Part II Comparison with database", *Int. J. Heat Mass Transfer* 47, 3387–3401 (2004).
- [9] W. Zhang, T. Hibiki, and K. Mishima, "Correlation for flow boiling heat transfer in mini-channels", *Int. J. Heat Mass Transfer* 47, 5749–5763 (2004).
- [10] J. Lee and I. Mudawar, "Two-phase flow in high-heat-flux micro-channel heat sink for refrigeration cooling applications. Part I: pressure drop characteristics", *Int. J. Heat Mass Transfer* 48, 928–940 (2005).
- [11] G. Hetsroni, A. Mosyak, Z. Segal, and E. Pogrebnyak, "Two-phase flow pattern in parallel micro-channels", *Int. J. Multiphase Flow* 29, 344–360 (2003).
- [12] G. Hetsroni, A. Mosyak, E. Pogrebnyak, and Z. Segal, "Explosive boiling of water in parallel micro-channels", *Int. J. Multiphase Flow* 31, 371–392 (2005).
- [13] G. Hetsroni, A. Mosyak, E. Pogrebnyak, and S. Segal, "Periodic boiling in parallel micro-channels at low vapor quality", *Int. J. Multiphase Flow* 32, 1141–1159 (2006).
- [14] L. Zhang, J-M. Koo, L. Jiang, M. Asheghi, K.E. Goodson, and J.K. Santiago, "Measurements and modelling of two-phase flow in micro-channels with nearly constant heat flux boundary conditions", *J. Microelectromech. Syst.* 11, 12–19 (2002).
- [15] M. Steinke, and S.G. Kandlikar, "An experimental investigation of flow boiling characteristics of water in parallel micro-channels", *Trans. ASME J. Heat Transfer* 126, 518–526 (2004).
- [16] S.G. Kandlikar, "Fundamental issues related to flow boiling in mini-channels and micro-channels", *Exp. Thermal Fluid Sci.* 26, 389–407 (2002).
- [17] H.J. Lee and S.Y. Lee, "Pressure drop correlations for two-phase flow within horizontal rectangular channels with small heights", *Int. J. Multiphase Flow* 27, 782–796 (2001).
- [18] H.C. Lee, B.D. Oh, S.W. Bae, and M.H. Kim, "Single bubble growth in saturated pool boiling on a constant wall temperature surface", *Int. J. Multiphase Flow* 29, 1857–1874 (2003).
- [19] A.E., Bergles and G.G., Kandlikar, "On the nature of critical heat flux in micro-channels", *J. Heat Transfer* 127, 101–107 (2005).
- [20] V.K. Dhir, "Boiling heat transfer", *Ann. Rev. Fluid Mech.* 30, 365–401 (1998).
- [21] P.C. Lee, F.C. Tseng, and C. Pan, "Bubble dynamics in microchannels. Part 1: Single microchannel", *Int. J. Heat Mass Transfer* 47, 5575–5589 (2004).
- [22] H.Y. Li, F.C. Tseng, and C. Pan, "Bubble dynamics in micro-channels. Part II: two parallel micro-channels", *Int. J. Heat Mass Transfer* 47, 5591–5601 (2004).
- [23] L.P. Yarin, A. Mosyak, and G. Hetsroni, *Fluid Flow, Heat Transfer and Boiling in Micro-channels*, Springer Verlag, Berlin, 2008.
- [24] V. Prodanovic, D. Fraser, and M. Salcudean, "On transition from partial to fully developed subcooled flow boiling", *Int. J. Heat Mass Transfer* 45, 4727–4738 (2002).
- [25] B. Agostini, J.R. Thome, M. Fabbri, B. Michel, D. Calmi, and U. Kloter, "High heat flux flow boiling in silicon multi-micro-channels. Part I: Heat transfer characteristics of re-

## Boiling in micro-channels

- frigerant R236fa”, *Int. J. Heat Mass Transfer* 51, 5400–5414 (2008).
- [26] R. Revellin and J. Thome, “A theoretical model for the prediction of the critical heat flux in heated micro-channel”, *Int. J. Heat and Mass Transfer* 51, 1216–1225 (2008).
- [27] S.G. Kandlikar, “Nucleation characteristics and stability considerations during flow boiling in micro-channels”, *Exp. Thermal and Fluid Science* 30, 441–447 (2006).
- [28] S. Kakac and B. Bon, “A review of two-phase flow dynamic instabilities in tube boiling systems”, *Int. J. Heat Mass Transfer* 51, 399–433 (2008).
- [29] G. Wang, P. Cheng, and A.E. Bergles, “Effects of inlet outlet configurations on flow boiling instability in parallel micro-channels”, *Int. J. Mass Transfer* 51, 2267–2281 (2008).
- [30] H.J. Lee and S.Y. Lee, “Heat transfer correlation for boiling flows in small rectangular horizontal channels with low aspect ratios”, *Int. J. Multiphase Flow* 27, 2043–2062 (2001).
- [31] T-H. Yen, N. Kasagi, and Y. Suzuki, “Forced convective boiling heat transfer in micro-tubes at low mass and heat fluxes”, *Int. J. Multiphase Flow* 29, 1771–1792 (2003).
- [32] S. Grohmann, “Measurement and modeling of single-phase and flow-boiling heat transfer in micro-tubes”, *Int. J. Heat Mass Transfer* 48, 4072–4089 (2005).
- [33] T-H. Yen, M. Shji, F. Takemura, Y. Suzuki, and N. Kasagi, “Visualization of convective boiling heat transfer in single micro-channels with different shaped cross-sections”, *Int. J. Heat Mass Transfer* 49, 3884–3894 (2006).
- [34] J. Lee and I. Mudawar, “Two-phase flow in high-heat-flux micro-channel heat sink for refrigeration cooling applications. Part II: heat transfer characteristics”, *Int. J. Heat Mass Transfer* 48, 941–955 (2005).
- [35] W. Zhang, T. Hibiki, K. Mishima, and Y. Mi, “Correlation of critical heat flux for flow boiling of water in mini-channels”, *Int. J. Heat and Mass Transfer* 49, 1058–1072 (2006).
- [36] D.D. Hall and I. Mudawar, “Critical heat flux (CHF) for water flow in tubes—II. Subcooled CHF correlations”, *Int. J. Heat Mass Transfer* 43, 2605–2640 (2000).
- [37] L. Wojtan, R. Revellin, and J. Thome, “Investigation of critical heat flux in single uniformly heated micro-channels”, *Exp. Therm. Fluid Sci.* 30, 765–774 (2006).
- [38] W. Qu and I. Mudawar, “Measurement and correlation of critical heat flux in two-phase micro-channel heat sinks”, *Int. J. Heat Mass Transfer* 47, 2045–2059 (2004).
- [39] M.B. Bowers and I. Mudawar, “High flux boiling in low flow rate, low pressure drop mini-channel and micro-channel heat sinks”, *Int. J. Heat Mass Transfer* 37, 321–332 (1994).
- [40] G.M. Lazarek and S.H. Black, “Evaporative heat transfer, pressure drop and critical heat flux in a small vertical tube with R-113”, *Int. J. Heat Mass Transfer* 25, 945–959 (1982).
- [41] K. Moriyama and A. Inoue, “Thickness of the liquid film formed by growing bubble in a narrow gap between two horizontal plates”, *J. Heat Transfer Trans ASME* 118, 132–139 (1996).